THE JOURNAL OF IMMUNOLOGY

The Role of Sphingosine-1-Phosphate Transporter *Spns2* in Immune System Function

Anastasia Nijnik, Simon Clare, Christine Hale, Jing Chen, Claire Raisen, Lynda Mottram, Mark Lucas, Jeanne Estabel, Edward Ryder, Hibret Adissu, Sanger Mouse Genetics Project, Niels C. Adams, Ramiro Ramirez-Solis, Jacqueline K. White, Karen P. Steel, Gordon Dougan and Robert E. W. Hancock

Supplementary Material	http://www.jimmunol.org/content/suppl/2012/06/04/jimmunol.1200282.DC1.html
Subscriptions	Information about subscribing to *The Journal of Immunology* is online at: http://jimmunol.org/subscriptions
Permissions	Submit copyright permission requests at: http://www.aai.org/ji/copyright.html
Email Alerts	Receive free email-alerts when new articles cite this article. Sign up at: http://jimmunol.org/cgi/alerts/etoc

The Role of Sphingosine-1-Phosphate Transporter *Spns2* in Immune System Function

Anastasia Nijnik,*,† Simon Clare,* Christine Hale,* Jing Chen,* Claire Raisen,* Lynda Mottram,* Mark Lucas,* Jeanne Estabel,* Edward Ryder,* Hibret Adissu,‡ Sanger Mouse Genetics Project,[1] Niels C. Adams,* Ramiro Ramirez-Solis,* Jacqueline K. White,* Karen P. Steel,* Gordon Dougan,* and Robert E. W. Hancock†

Sphingosine-1-phosphate (S1P) is lipid messenger involved in the regulation of embryonic development, immune system functions, and many other physiological processes. However, the mechanisms of S1P transport across cellular membranes remain poorly understood, with several ATP-binding cassette family members and the spinster 2 (Spns2) member of the major facilitator superfamily known to mediate S1P transport in cell culture. Spns2 was also shown to control S1P activities in zebrafish in vivo and to play a critical role in zebrafish cardiovascular development. However, the in vivo roles of Spns2 in mammals and its involvement in the different S1P-dependent physiological processes have not been investigated. In this study, we characterized *Spns2*-null mouse line carrying the *Spns2*^tm1a(KOMP)Wtsi allele (*Spns2*^tm1a). The *Spns2*^tm1a/tm1a animals were viable, indicating a divergence in Spns2 function from its zebrafish ortholog. However, the immunological phenotype of the *Spns2*^tm1a/tm1a mice closely mimicked the phenotypes of partial S1P deficiency and impaired S1P-dependent lymphocyte trafficking, with a depletion of lymphocytes in circulation, an increase in mature single-positive T cells in the thymus, and a selective reduction in mature B cells in the spleen and bone marrow. Spns2 activity in the nonhematopoietic cells was critical for normal lymphocyte development and localization. Overall, *Spns2*^tm1a/tm1a resulted in impaired humoral immune responses to immunization. This study thus demonstrated a physiological role for Spns2 in mammalian immune system functions but not in cardiovascular development. Other components of the S1P signaling network are investigated as drug targets for immunosuppressive therapy, but the selective action of Spns2 may present an advantage in this regard. *The Journal of Immunology*, 2012, 189: 000–000.

L ipid messenger sphingosine-1-phosphate (S1P) is essential for normal embryonic development and the functions of the cardiovascular and immune systems (1), and components of the S1P signaling network are widely investigated as drug targets for suppression of transplant rejection, autoimmunity, and sepsis (2). In the extracellular environment S1P acts through five G protein coupled receptors ($S1P_{1-5}$) expressed on a variety of cell types (reviewed in Refs. 3, 4). In particular, the loss of S1P receptor 1 ($S1P_1$) results in embryonic lethality with abnormal development of the cardiovascular system, whereas a lymphocyte-specific loss of $S1P_1$ causes impaired exit of mature T cells out of the thymus (5, 6), B cells out of the bone marrow (7, 8), as well as a severe defect in lymphocyte egress from secondary lymphoid organs during their physiological recirculation (9, 10). $S1P_1$ is also required for normal localization of marginal zone B cells (11), B1 cells (12), plasma cells (13), and gut intraepithelial T lymphocytes (14), whereas S1P receptor 5 controls NK cell migration (15). Intracellular activities of S1P as a second-messenger molecule are broadly linked to cell survival and growth (16), and in the immune system intracellular S1P promotes inflammatory and antimicrobial activities of mast cells, macrophages, and neutrophils (17–22). In particular, S1P is produced downstream of FcεR crosslinking and stimulates mast cell degranulation (23, 24). It is also produced downstream of TNFR signaling and is required for TNFR-associated factor 2-dependent RIP1 activation and NF-κB signaling (25). These activities of S1P have been implicated in the pathologies of allergic and inflammatory disorders (26, 27).

The activities of S1P as a chemokine and a second messenger are critically dependent on the S1P concentrations in the different cellular compartments, the tissue environment, and the circulation, and these are established through the controlled rates of S1P production, degradation, and transport. S1P is synthesized by the sphingosine kinases, sphingosine kinase (SphK)1 and SphK2 (28–30), and it is degraded by the S1P lyase and S1P phosphatases (1, 31). Combined loss of SphK1 and SphK2 in mice results in embryonic lethality with abnormal cardiovascular development, whereas the loss of S1P lyase causes a milder phenotype with impaired lymphocyte egress from lymphoid organs. In contrast, the mechanisms of S1P transport across cellular membranes remain poorly understood. Several proteins of the ATP-binding cassette (ABC) transporter superfamily can mediate S1P secretion in cell culture, for example ABCC1 in mast cells (32), ABCA1 in RBCs (33), and another family member in platelets

---

*Wellcome Trust Sanger Institute, Hinxton, Cambridge CB10 1SA, United Kingdom; †Department of Microbiology and Immunology, University of British Columbia, Vancouver, British Columbia V6T 1Z4, Canada; and ‡Toronto Centre for Phenogenomics, Toronto, Ontario M5T 3H7, Canada

[1]All authors and their affiliations appear at the end of this article.

Address correspondence and reprint requests to Dr. Anastasia Nijnik, Department of Physiology, McGill University, 3649 Promenade Sir William Osler, Room 368, Bellini Building, Montreal, Quebec H3G 0B1, Canada. E-mail address: anastasiya.nyzhnyk@mcgill.ca

The online version of this article contains supplemental material.

Abbreviations used in this article: ABC, ATP-binding cassette; BMDM, bone marrow-derived macrophage; qPCR, quantitative PCR; S1P, sphingosine-1-phosphate; $S1P_1$, sphingosine-1-phosphate receptor 1; SphK, sphingosine kinase; Spns2, spinster homolog 2; TetC, tetanus toxin fragment C recombinant protein.

(34). Expression of the cystic fibrosis transmembrane conductance regulator on epithelial cell lines was also shown to contribute to S1P transport (35). However, knockout mice for these proteins do not phenocopy the knockouts of known S1P signaling network components, and plasma S1P levels in the mice lacking ABCA1 and ABCC1 are unaltered (36). Some S1P is also produced extracellularly by the extracellular SphK1 enzyme released from the vascular endothelium (37).

Spinster homolog 2 (Spns2) is a member of the major facilitator superfamily of transmembrane proteins (38). In recent studies, zebrafish Spns2 was shown to mediate S1P secretion, and the loss of Spns2 activity resulted in lethal defects in cardiovascular development (39, 40), similar to the phenotypes of the $SphK1^{-/-}$ $SphK2^{-/-}$ and $S1P_1^{-/-}$ mouse lines (30, 41). The human Spns2 protein was also shown to mediate the secretion of S1P as well as of S1P receptor agonist and immunosuppressive drug phospho-FTY720 (42). Furthermore, human Spns2 expression could rescue the developmental defects in zebrafish embryos (39). However, the in vivo functions of Spns2 in the mammalian system have not been investigated.

In the present work we characterized an *Spns2*-targeted mouse line *Spns2*[tm1a/tm1a] generated by the Wellcome Trust Sanger Institute as part of the International Knockout Mouse Consortium, and we demonstrate the requirement for Spns2 for the normal lymphocyte localization and mammalian immune system function but not the other S1P-mediated functions such as embryonic viability and cardiovascular development.

Materials and Methods

Gene targeting and mouse production

The mouse strain carrying the *Spns2*[tm1a(KOMP)Wtsi] allele was generated by blastocyst injection of embryonic stem cell clone EPD0090_5_B04 obtained from the Knockout Mouse Project resource (43). Prior to microinjection, the identity of the targeted embryonic stem cells was verified by 5′ long-range PCR using a primer external to the targeting vector. Chimeric mice were bred to C57BL/6-*Tyr*[c-Brd] and germline transmission was verified by quantitative PCR (qPCR) to detect the neo transgene included in the mutant allele (single insertion event), as well as by loss of wild-type allele qPCR (correct targeted locus) in the F_1 heterozygous mice. The presence of the downstream LoxP site was verified by PCR. The C57BL/6N-*Hprt*[Tg(CMV-cre)Brd/Wtsi] and C57BL/6N-Gt(ROSA)26Sor[tm1(FLP1)Dym/Wtsi] transgenic lines with systemic expression of Cre and Flp recombinases were previously described (44, 45). The *Spns2*[tm1b(KOMP)Wtsi] allele was generated by crossing the tm1a allele to the C57BL/6N-*Hprt*[Tg(CMV-Cre)Brd] allele to delete exon 3 and the neo cassette between the LoxP sites, and the Cre allele was bred out of the colony before study. The *Spns2*[tm1c(KOMP)Wtsi] allele was generated by breeding to C57BL/6N-Gt(ROSA)26Sor[tm1(FLP1)Dym/Wtsi] (*Rosa26*[Fki]) allele expressing Flp recombinase ubiquitously, to delete the inserted cassette but retaining exon 3 flanked by LoxP sites. All of the studies were performed on a C57BL/6 genetic background. The mice were maintained in specific pathogen-free conditions, and matched by age and sex within experiments. The care and use of all mice was in accordance with U.K. Home Office regulations, U.K. Animals Scientific Procedures Act 1986.

RNA isolation and qPCR

For the comparisons of *Spns2* transcript levels in wild-type and *Spns2*[tm1a/tm1a] tissues (Fig. 1B) RT-qPCR was performed using an RNA-to-Ct 1-Step kit (Applied Biosystems) in a 10 μl reaction with 1 μl total RNA (20–500 ng depending on tissue type). A TaqMan assay (Mm01249325) spanning the exons flanking the splice acceptor site of the construct was used in a multiplex reaction with a GAPDH endogenous control to normalize for variations between the amounts of input RNA (Applied Biosystems), and amplified in triplicate using a ViiA 7 qPCR machine (Applied Biosystems). Analysis was performed using the ViiA 7 1.1 analysis software and the ΔΔCt relative quantification module. For the comparisons of *Spns2* transcript levels across different tissues of wild-type mice (Fig. 5A), RNA was isolated using the RNeasy Plus Mini kit (Qiagen) and reverse-transcribed with the QuantiTect reverse transcription kit (Qiagen). qPCRs were performed using the QuantiTect SYBR Green PCR Kit (Qiagen), using *Spns2* QuantiTect primer assay (Qiagen) and *Actb* primers 5′-CTAAGGCCAACCGTGAAAAG-3′

(forward) and 5′-ACCAGAGGCATACAGGGACA-3′ (reverse) (Sigma-Aldrich). The *Spns2* primers spanned the boundaries of exons 5–7 of the *Spns2* coding transcript ENSMUST00000045303. The data were acquired on the StepOnePlus real-time PCR system (Applied Biosystems) and analyzed using the ΔΔCt method.

Flow cytometry

Cell suspensions of mouse tissues were prepared in RPMI 1640 with 2% (v/v) FCS (Sigma-Aldrich), 100 μg/ml streptomycin, and 100 U/ml penicillin (all from Invitrogen). Blood was collected into heparin-coated tubes (Kabe Labotechnik) by cardiac puncture, and erythrocytes were lysed using PharmaLyse (BD Biosciences). The cells were stained in PBS with 2% FCS (Sigma-Aldrich) and 0.2% (w/v) sodium azide (Sigma-Aldrich) for 20 min on ice, with the following Abs. Fluorescein-conjugated Abs were against CD4 (clone L3T4), CD8 (53-6.7), CD11b (M1/70), CD21 (7G6), CD86 (GL1), and B220 (RA3-6B2; all from BD Pharmingen). PE-conjugated Abs were against CD8 (clone 53-6.7), CD19 (1D3), CD69 (H1.2F3), CD80 (16-10A1), and IgM (R6-60.2; all from BD Pharmingen). Allophycocyanin-conjugated Abs were against CD4 (RM4-5), CD8 (53-6.7), and CD44 (IM7; all from BD Pharmingen). Allophycocyanin-Cy7 Abs were against CD8 (53-6.7), CD11b (M1/70; both from BioLegend), and B220 (RA3-6B2; from BD Pharmingen). PerCP-conjugated anti-CD45.1 (A20; BioLegend), Alexa Fluor 647-conjugated anti-IgD (clone 11-26; eBioscience), and PE-Cy7 anti-CD23 (B3B4; eBioscience) were also used. Flow cytometric measurements of β-galactosidase activity were performed using FluoReporter lacZ flow cytometry kits (Invitrogen/Molecular Probes). The cells were stained for appropriate combinations of cell surface lineage markers, before loading with fluorescein di-β-D-galactopyranoside and analysis by flow cytometry. The data were acquired on BD FACSAria or LSRII flow cytometers and analyzed with FACSDiva software.

ELISA

For the measurements of Ab levels, mouse blood was collected by tail bleed or cardiac puncture, and serum was prepared and stored at −20°C. For Ag-specific Ab measurements in mouse serum, Nunc MaxiSorp plates were coated overnight at 4°C with 2 mg/ml tetanus toxin fragment C recombinant protein (TetC) in 0.1 M Na₂HPO₄ (pH 9.0), blocked with 3% (w/v) BSA in PBS for 1 h, and incubated with 5-fold serial dilutions of mouse serum in PBS with 1% BSA for 1 h. The plates were developed with anti-mouse IgG, IgG_1, or IgG_{2a} HRP-conjugated Abs (BD Pharmingen), followed by *o*-phenylenediamine substrate tablets (Sigma-Aldrich) dissolved in water. Cytokine ELISA on cell culture supernatants was performed using anti-mouse TNF-α–coating Ab clone 1F3F3D4 and biotin-conjugated detection Ab clone XT3/XT22, followed by avidin HRP (all from eBioscience), and the 3,3′,5,5′-tetramethylbenzidine liquid substrate system (Sigma-Aldrich). Absorbances were measured using the Bio-Rad 680 microplate reader.

Measurements of S1P levels and activity

For the measurements of S1P levels, mouse blood was collected from the retro-orbital sinus. S1P levels in the plasma were measured using the ELISA-based S1P assay kit (Echelon Biosciences) according to the manufacturer's protocol. Assays of S1P activity in mouse plasma used an $S1P_1$ redistribution assay (Thermo Scientific) according to the manufacturer's instructions. Briefly, the assay measured S1P-induced internalization of $S1P_1$, when mouse plasma is added at different dilutions to the U2OS cells stably expressing GFP-tagged $S1P_1$. Internalization of $S1P_1$-GFP was quantified using the spot detection algorithm and the "spot total area per object" function on Cellomics ArrayScan VTI system. S1P (Cayman Chemicals) was used to prepare the positive controls.

Mouse immunization

Recipient mice were immunized by intranasal inhalation of 30 μl PBS containing 10 mg TetC (gift from Omar Qazi, Imperial College) combined with 1 mg heat-labile toxin of *Escherichia coli* (gift of Rino Rappuoli, Chiron) adjuvant. Mice were boosted on days 7, 21, and 37. Serum samples were collected on days 36 and 40. Detection of TetC-specific Abs from sera was performed by ELISA as described above.

Mouse bone marrow transfer experiments

Recipient animals were irradiated with two doses of 4.5 Gy, 3 h apart, and injected i.v. with 3×10^6 donor bone marrow cells. The mice were maintained on clindamycin (250 mg/l) in drinking water for 2 wk and analyzed 8 wk after reconstitution. In one experiment *Spns2*[tm1a/tm1a] and *Spns2*[+/tm1a] recipients were reconstituted either with wild-type CD45.1⁺-marked or with *Spns2*[tm1a/tm1a] donor bone marrow. In a separate study

$Spns2^{+/+}Rag1^{-/-}$ recipients were reconstituted with wild-type CD45.1$^+$-marked bone marrow and $Spns2^{tm1a/tm1a}$ bone marrow, either separately or together, mixed in 1:1 ratio. Using CD45.1$^+$-marked wild-type donor bone marrow we confirmed that this protocol results in a complete replacement of the hematopoietic system of the recipients, so that >95% of the hematopoietic progenitors, bone marrow cells of all hematopoietic lineages, as well as thymocytes were donor derived (data not shown).

Tissue culture

Bone marrow-derived macrophages (BMDMs) were generated by culturing mouse bone marrow for 6 d in high-glucose DMEM (Invitrogen) supplemented with 20% (v/v) FCS (Sigma-Aldrich), 25% (v/v) L-conditioned media (supernatant of cell line L-929), 2 mM L-glutamine, 1 mM sodium pyruvate, 100 µg/ml streptomycin, and 100 U/ml penicillin (all from Invitrogen). The cells were maintained at 37˚C and 5% CO_2 in a humidified incubator. For stimulation the cells were replated at 1×10^6/ml and treated with 100 ng/ml LPS (Sigma-Aldrich), 25 ng/ml IFN-γ (R&D Systems), and/or 25 ng/ml TNF-α (eBioscience) over a 48-h time course.

Tissue staining for β-galactosidase activity

Mice were fixed by cardiac perfusion with 4% (w/v) paraformaldehyde. Following dissection, the tissues were fixed in 4% paraformaldehyde for a further 30 min, rinsed in PBS, and stained in 0.1% (w/v) 5-bromo-4-chloro-3-indolyl-β-D-galactoside (X-Gal; Invitrogen) for up to 48 h. After an additional overnight fixation in 4% paraformaldehyde, the tissues were cleared with 50% (v/v) glycerol and transferred to 70% glycerol for long-term storage. Images were taken using a Leica MZ16A microscope and iMagic software.

Statistical analyses

Statistical comparisons were performed with Prism 4.0 software (GraphPad Software) using a two-tailed Student t test or nonparametric Mann–Whitney U test for comparisons of two datasets, and ANOVA was used for multiple comparisons.

Results

Spns2 gene targeting and mouse production

$Spns2$ gene targeting was carried out as part of the International Knockout Mouse Consortium, in the JM8 embryonic stem cell line on a C57BL/6N genetic background (43). The targeted $Spns2^{tm1a(KOMP)WTSI}$ allele carried a gene-trap DNA cassette, inserted into the second intron of the gene, consisting of a splice acceptor site, an internal ribosome entry site, and a β-galactosidase reporter, followed by a neomycin resistance marker expressed from an independent β-actin promoter (Fig. 1A; GenBank file available at http://www.knockoutmouse.org). The use of the splice acceptor site in the cassette is predicted to generate a truncated nonfunctional transcript encoding the first 145 of 549 aas of the Spns2 protein, including only 1 of the 11 predicted Spns2 transmembrane α-helices (prediction using Swiss EMBNet, available at http://www.ch.embnet.org/). Quantitative RT-PCR (qRT-PCR) analysis of $Spns2^{tm1a/tm1a}$ mouse tissues (liver, lung, spleen, and mesenteric lymph nodes) confirmed that the targeted allele effectively disrupted the production of $Spns2$-coding mRNA, with a 200- to 1000-fold reduction in the levels of the transcript containing the junction of exons 2–3 of $Spns2$ mRNA ENSMUST00000045303 in the different tissues analyzed (Fig. 1B). The locations of the $LoxP$ and Frt sites are designed to allow the conversion of the allele to a conditional configuration in future studies (43).

The $Spns2^{tm1a/tm1a}$ mice were profiled using a series of high-throughput phenotype screens, under the scope of the Sanger Institute Mouse Genetics Project, with the full information available at http://www.sanger.ac.uk/mouseportal/search?query=spns2. The $Spns2^{tm1a/tm1a}$ animals showed no significant increase in the levels of embryonic mortality in strong contrast to the previously characterized embryonic lethal $SphK1^{-/-}SphK2^{-/-}$ and $S1P_1^{-/-}$ mouse lines (30, 41). The $Spns2^{tm1a/tm1a}$ mice also showed no gross dysmorphology, apart from abnormal eye pigmentation and opacity, and they were able to breed normally. In particular, these mice demonstrated no alterations in heart weight or histology at 16 wk age, in strong contrast to $Spns2^{-/-}$ zebrafish that exhibited defects in embryonic heart development (cardia bifida) (39, 40), as well as $SphK1^{-/-}SphK2^{-/-}$ mice that demonstrated poor embryonic development of the dorsal aorta (30). Abnormalities in the immune phenotype of the $Spns2^{tm1a/tm1a}$ line were analyzed in this study, whereas the phenotypes of the ear and eye will be reported elsewhere (J. Chen and K.P. Steel, manuscript in preparation).

Abnormal T and B lymphocyte development and localization in Spns2$^{tm1a/tm1a}$ mice

To establish the impact of $Spns2^{tm1a/tm1a}$ on lymphocyte development and localization, the blood and lymphoid organs of $Spns2^{tm1a/tm1a}$ mice were analyzed. We observed a reduction in the overall leukocyte counts in $Spns2^{tm1a/tm1a}$ mouse blood (3.38×10^3/µl in $Spns2^{tm1a/tm1a}$ versus 6.63×10^3/µl in the wild-type mice; Supplemental Fig. 1A), whereas erythrocyte and platelet counts were not affected (data not shown). The percentage of CD4 and CD8 lineage T cells in the blood and the absolute numbers of CD4 and CD8 T cells in the spleen of $Spns2^{tm1a/tm1a}$ mice were significantly reduced (~4-fold; Fig. 2A). This was accompanied by a moderate increase in the proportion of mature CD4 and CD8 single-positive T cells in the thymus (Fig. 2B, 2C), with the CD4$^+$ CD8$^-$ cells constituting 12 ± 0.9% of thymocytes in $Spns2^{tm1a/tm1a}$ as compared with 7 ± 0.5% in wild-type mice (mean $\pm$ SD). The thymic CD4$^+$CD8$^-$ and CD4$^-$CD8$^+$ $Spns2^{tm1a/tm1a}$ T cells expressed lower levels of CD24 and CD69 and higher levels of CD62L, indicating their more mature status (Fig. 2D, 2E). These features closely resemble the phenotypes of other mouse lines with defects in S1P production, turnover, or sensing (5, 6, 31, 46), indicating an accumulation of mature T cells in the thymus and suggesting a defect in T cell recruitment from the thymus into the
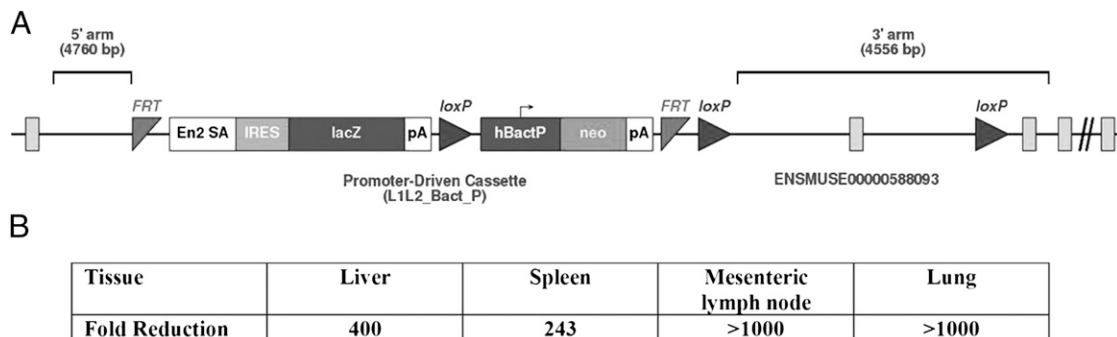

FIGURE 1. $Spns2$ gene targeting. (**A**) Structure of the $Spns2^{tm1a(KOMP)WTSI}$ ($Spns2^{tm1a}$) allele. (**B**) Average fold reduction in $Spns2$ transcript levels in $Spns2^{tm1a/tm1a}$ relative to wild-type tissues (liver, spleen, lymph nodes, and lung), analyzed by qRT-PCR using primers spanning the junction of exons 2–3 of the $Spns2$ coding transcript ENSMUST00000045303.
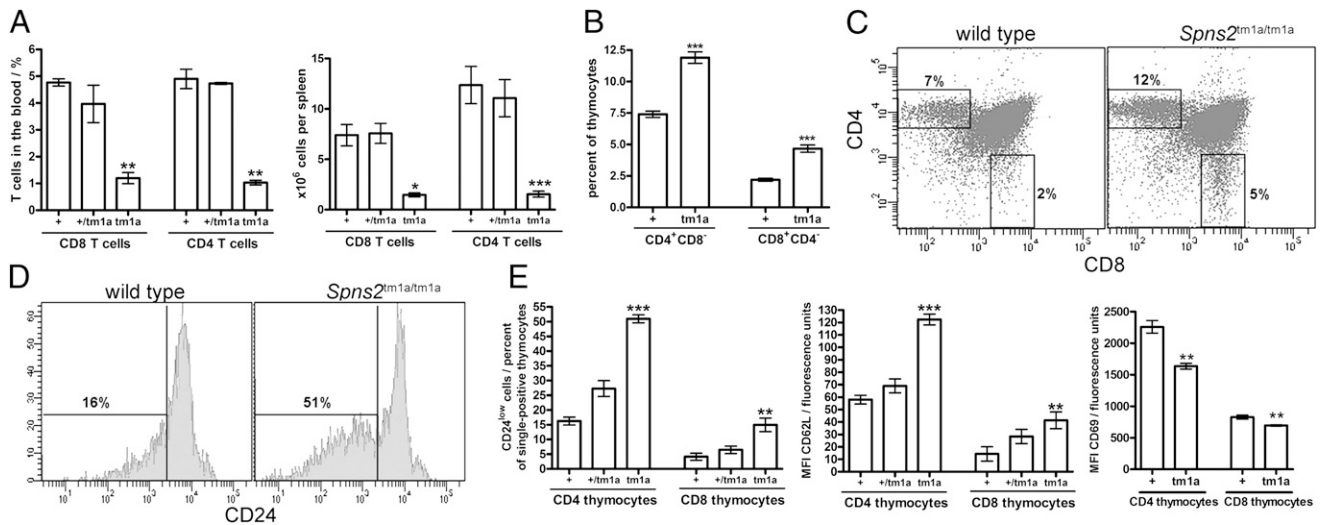
Tissue	Liver	Spleen	Mesenteric lymph node	Lung
Fold Reduction	400	243	>1000	>1000

FIGURE 2. T cell abnormalities in the *Spns2*[tm1a/tm1a] mice. (**A**) Percentage of CD4 and CD8 T cells in the blood and numbers of CD4 and CD8 T cells in the spleen of wild-type, *Spns2*[+/tm1a], and *Spns2*[tm1a/tm1a] mice (+, +/tm1a, and tm1a, respectively). (**B**) Percentage of CD4^{+} and CD8^{+} single-positive cells in the thymus of wild-type, *Spns2*[+/tm1a], and *Spns2*[tm1a/tm1a] mice (+, +/tm1a, and tm1a, respectively). (**C**) Representative flow cytometry plots of wild-type and *Spns2*[tm1a/tm1a] thymocytes stained for CD4 and CD8; average percentage of cells within the CD4^{+} and CD8^{+} single-positive gates is indicated. (**D**) Representative flow cytometry histograms indicating CD24 expression on CD4^{+} single-positive thymocytes in wild-type and *Spns2*[tm1a/tm1a] mice. (**E**) Percentage of CD24^{low} cells within the CD4^{+} and CD8^{+} single-positive thymocyte gates; the expression of CD62L and CD69 on CD4^{+} and CD8^{+} single-positive thymocytes in wild type (+), *Spns2*[+/tm1a] (+/tm1a), and *Spns2*[tm1a/tm1a] (tm1a) mice is indicated. Bars represent means ± SEM. MFI, mean fluorescence intensity. Data are from three to four mice per group and were reproducible in two independent experiments. *$p < 0.05$, **$p < 0.01$, ***$p < 0.001$ using ANOVA with a Bonferroni post hoc test or *t* test.

circulation. There were no abnormalities in the numbers of the earlier thymocyte subsets, including CD4^{−}CD8^{−} double-negative thymocytes (subsets 1–4, differentiated by CD44 and CD25 expression) and CD4^{+}CD8^{+} double-positive thymocytes (data not shown).

There was also a significant reduction in the number of recirculating B cells in *Spns2*[tm1a/tm1a] mice (CD45^{+}CD19^{+}; Fig. 3A). This was accompanied by a reduction in the follicular B cell population in the spleen (gated as B220^{+}IgM^{+}IgD^{+} or B220^{+}CD23^{+}CD21^{low}; Fig. 3B–D) and the mature B cell population in the bone marrow (B220^{+}IgM^{+}IgD^{+}; Fig. 3E). In contrast, no abnormalities in earlier B cell developmental subsets were observed, with normal numbers of pro/pre-B cells (B220^{+}IgM^{−}IgD^{−}) and immature B cells (B220^{+}IgM^{+}IgD^{−}) in the bone marrow and transitional B cells (B220^{+}CD23^{low}CD21^{low}) in the spleen of the *Spns2*[tm1a/tm1a] mice (Fig. 3D, 3E). Overall, this phenotype resembles the loss of recirculating and mature follicular B cell population previously reported in other mouse lines with impaired S1P production or sensing (5, 31, 46). We also observed a reduction in the numbers of B1 cells in the peritoneal cavity of *Spns2*[tm1a/tm1a] mice (B220[low]IgM[high]IgD[low]; data not shown), consistent with the role of S1P in the control of their trafficking (12).

Reduced Ab responses to immunization in Spns2[tm1a/tm1a] *mice*

To establish whether the defects in lymphocyte development and localization seen in the *Spns2*[tm1a/tm1a] mice led to impaired Ab responses to immune challenge, the mice were immunized intranasally with TetC, boosted at days 7 and 21, and analyzed for Ag-specific Ab titers in the serum at day 36. Significant reductions in Ag-specific total IgG and IgG[1] were seen (Fig. 4), indicating impaired humoral immunity in the *Spns2*[tm1a/tm1a] mouse line. The mice were subsequently given a tertiary boost, and serum Ab levels were measured again 3 d later (day 40), confirming the reduction in Ag-specific total IgG and IgG[1] in *Spns2*[tm1a/tm1a] mice (data not shown). However, the levels of IgG[2a] were not significantly reduced (Fig. 4), and this might have been due to the low

levels and high variation in IgG[2a] production in both the wild-type and *Spns2*[tm1a/tm1a] groups.

Normal macrophage responses to inflammatory stimuli in Spns2[tm1a/tm1a] *mice*

S1P functions not only as a chemoattractant in the extracellular environment, but also as an intracellular messenger required for the normal signaling downstream of TNFR and TLRs (25); furthermore inhibition of S1P production is protective in animal models of endotoxemia and sepsis (26). To establish whether *Spns2*[tm1a/tm1a] disrupted normal cellular responses to TLR and TNFR stimulation, BMDMs, generated from *Spns2*[tm1a/tm1a] and wild-type control mice, were stimulated with LPS (100 ng/ml), IFN-γ (25 ng/ml), and/or TNF-α (25 ng/ml) and analyzed for induction of CD80 and CD86 activation markers and secretion of inflammatory cytokines. No differences in the responses of *Spns2*[tm1a/tm1a] and wild-type cells were observed (Supplemental Fig. 1B). This suggests that Spns2 does not affect intracellular S1P functions in macrophages downstream of TLR or TNFR stimulation.

Cell-intrinsic activity of Spns2 *is dispensable for lymphocyte development and localization*

Many cell types have been shown to produce and release S1P, including erythrocytes, lymphatic and vascular endothelial cells, platelets, and mast cells (32, 34, 46–50). To assess Spns2 expression in a broad range of mammalian cell types, a range of tissues and organs from *Spns2*[+/tm1a] mice were profiled for the activity of the β-galactosidase reporter expressed from the endogenous *Spns2* promoter in mice carrying the *Spns2*[tm1a] allele (51). The studies were done as part of the Sanger Mouse Genetics Project high-throughput phenotyping, and the data on the β-galactosidase reporter activity in 39 organs and tissues of *Spns2*[+/tm1a] mice is summarized in Supplemental Table I, with images available at http://www.sanger.ac.uk/mouseportal/phenotyping/MBNZ/adult-lac-z-expression. The expression of the *Spns2* gene was further confirmed in a selection of tissues using wild-type tissues
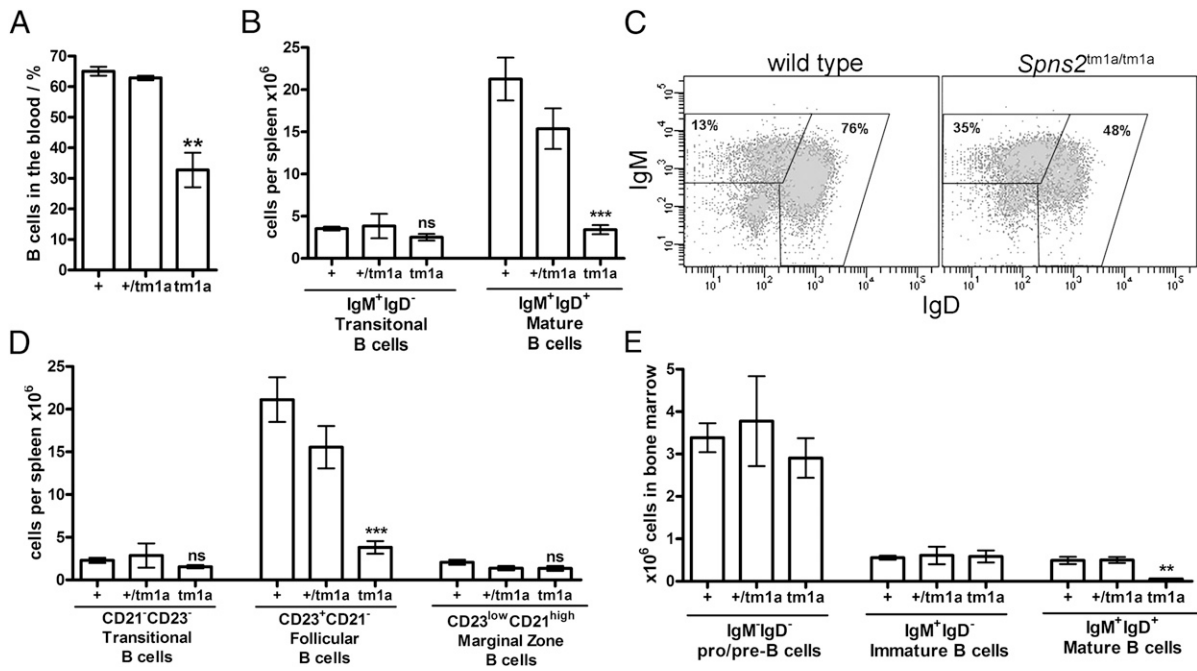
FIGURE 3. Reduction in the numbers of recirculating B cells in the blood and mature B cells in the spleen and bone marrow of $Spns2^{tm1a/tm1a}$ mice. (**A**) Reduction in the percentage of B cells (gated as CD45$^+$CD19$^+$) in the blood of $Spns2^{tm1a/tm1a}$ mice. (**B**) Reduction in the absolute number of mature B cells (gated as B220$^+$IgM$^+$IgD$^+$) in the spleen of $Spns2^{tm1a/tm1a}$ mice. (**C**) Representative flow cytometry plots of splenocytes, stained for B220, IgM, and IgD and gated on the B220$^+$ B cell population. Gates indicate IgM$^+$IgD$^-$ transitional and IgM$^+$IgD$^+$ mature B cells; the average percentage of cells within each gate for all mice in the group is indicated. (**D**) Reduction in the numbers of mature follicular B cells in the spleen of $Spns2^{tm1a/tm1a}$ mice confirmed by B220$^+$ CD21$^-$CD23$^+$ staining. (**E**) Reduction in mature B cells (B220$^+$IgM$^+$IgD$^+$) in the bone marrow of $Spns2^{tm1a/tm1a}$ mice. All bars represent means ± SEM. Data are from three mice per group and were reproducible in two independent experiments; bone marrow cell counts are per one tibia and femur. **$p <$ 0.01, ***$p <$ 0.001 using ANOVA with a Bonferroni post hoc test.

and qRT-PCR. Overall. it was demonstrated that there were high $Spns2$ transcript levels in the liver and lung, lower levels in the lymph nodes, spleen, and bone marrow, and low but detectable levels in the thymus (Fig. 5A).

To establish whether $Spns2$ was expressed in the lymphocyte populations affected by the $Spns2^{tm1a/tm1a}$ phenotype, $Spns2$ promoter-driven β-galactosidase reporter activity was analyzed in $Spns2^{+/tm1a}$ lymphocytes using flow cytometry with a fluorescent β-galactosidase substrate. The data showed no significant β-galactosidase activity over the background level in the different subpopulations of thymocytes or in splenic T cells (Fig. 5B), indicating that the $Spns2$ gene is not expressed in these cell types. The $Spns2$ gene was also not expressed in splenic B cells (Fig. 5B). As a positive control, high levels of β-galactosidase reporter activity were detected in hematopoietic cells of another mouse line $Mysm1^{+/tm1a}$ (52).

The requirement for Spns2 expression and activity in lymphocytes for their normal development and localization was further tested using bone marrow chimeras. Lethally irradiated $Spns2^{+/+}$ $Rag1^{-/-}$ recipients were reconstituted with a 50:50 mix of wild-type CD45.1$^+$-marked and $Spns2^{tm1a/tm1a}$ bone marrows and ana-

lyzed at 8 wk after reconstitution. No significant differences in the development and localization of wild-type and $Spns2^{tm1a/tm1a}$ lymphocytes were observed in this study. For example, ∼50% of CD4 and CD8 T cells in the blood and spleen of the chimeric mice were CD45.1$^-$ $Spns2^{tm1a/tm1a}$ (Fig. 5C). This demonstrated that $Spns2^{tm1a/tm1a}$ lymphocytes could develop and migrate normally when placed in a wild-type environment, and therefore that Spns2 expression in lymphocytes was dispensable for their normal development and localization. Additionally, an adoptive i.v. transfer of 10^7 $Spns2$ wild-type GFP-expressing splenocytes into either wild-type or $Spns2^{tm1a/tm1a}$ recipients demonstrated a significant reduction in the transferred CD4 T cells in the blood of $Spns2^{tm1a/tm1a}$ as compared with wild-type mice at 48 h, suggesting the role of the $Spns2^{tm1a/tm1a}$ environment in affecting CD4 T cell localization; however, no reduction in CD8 T cells and B cells was observed (data not shown).

Spns2 activity in the nonhematopoietic stromal cells is essential for normal immune function

The requirement for Spns2 expression and activity on different cell types for normal lymphocyte development and trafficking was

FIGURE 4. Impaired humoral immune response in the $Spns2^{tm1a/tm1a}$ mouse line. Wild-type (+/+) and $Spns2^{tm1a/tm1a}$ (tm1a/tm1a) mice were immunized intranasally with TetC, boosted at days 7 and 21, and analyzed for Ag-specific Ab titers in the serum at day 36. Bars represent means ± SEM. Data are from six mice per group. *$p <$ 0.05, **$p <$ 0.01 using a Student t test.
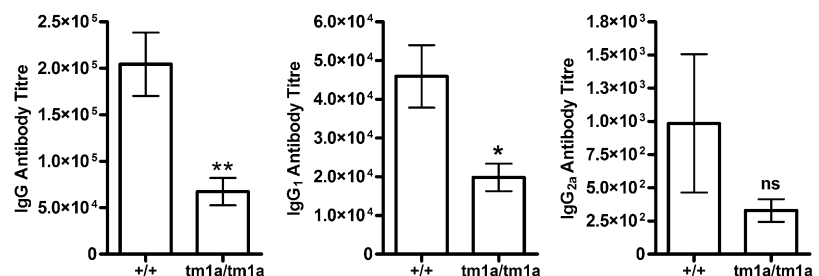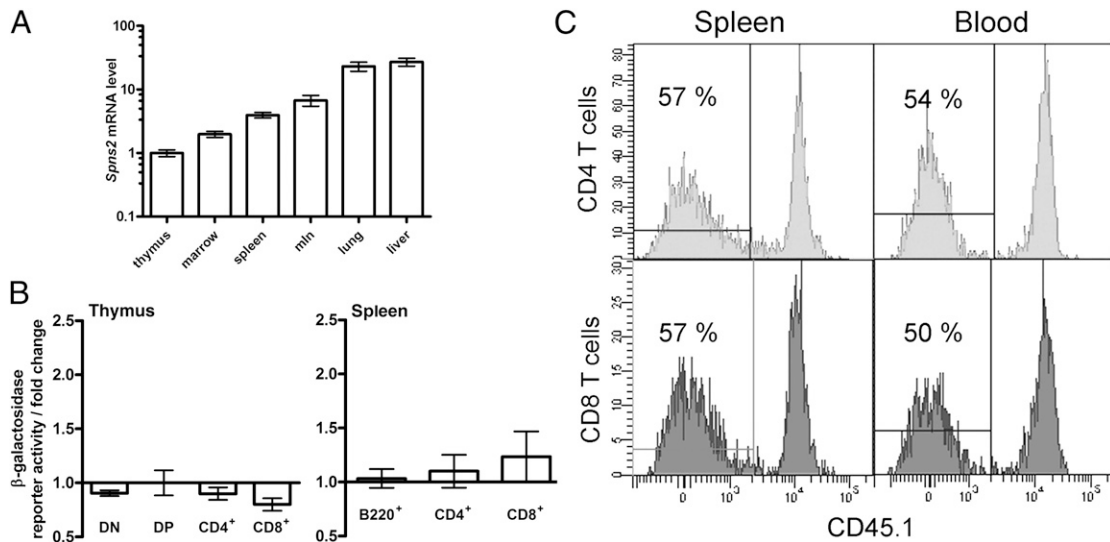
FIGURE 5. Analysis of *Spns2* expression. (**A**) qRT-PCR analysis of the *Spns2* transcript levels in the tissues of wild-type mice. Analysis using primers spanning exon junctions 5–7 of *Spns2* coding transcript ENSMUST00000045303. Data were analyzed using the $\Delta\Delta$Ct method with β-actin as the housekeeping control. *Spns2* transcript levels in the thymus were assigned the arbitrary value of 1 and the levels in other tissues were expressed relative to it. (**B**) β-galactosidase reporter activity in thymocytes, and splenic B and T cells, as a measure *Spns2* gene expression. The measurements were done in *Spns2*[+/tm1a] cells and are presented as fold change relative to the background β-galactosidase activity in the same cell type in wild-type mice. The cells were gated as: CD4^{−}CD8^{−} for double-negative thymocytes (DN), CD4^{+}CD8^{+} for double-positive thymocytes (DP), and B220^{+} for splenic B cells. Bars represent means ± SEM from three or more mice per group. (**C**) Mixed bone marrow chimeras, demonstrating that the defects in the development and localization of *Spns2*[tm1a/tm1a] T cells are not due to a cell-intrinsic requirement for Spns2. Lethally irradiated *Spns2*^{+/+}*Rag1*^{−/−} recipients were reconstituted with a 50:50 mix of wild-type CD45.1[+]-marked and *Spns2*[tm1a/tm1a] bone marrows. Flow cytometry histograms of CD4 and CD8 T cells in the spleen and blood at 8 wk following reconstitution are shown, and the percentage of C45.1[−] *Spns2*[tm1a/tm1a] T cells in each plot is indicated. mln, Mesenteric lymph nodes.

investigated further using bone marrow chimeras. Lethally irradiated recipients of *Spns2*[tm1a/tm1a] and *Spns2*[+/tm1a] genotypes were reconstituted either with wild-type (CD45.1[+]) or with *Spns2*[tm1a/tm1a] (CD45.1[−]) bone marrow and analyzed by flow cytometry at 8 wk after the reconstitution. The results indicated that the *Spns2* genotype of the nonhematopoietic cells was of primary importance for normal lymphocyte development in the chimeras. Thus, when the wild-type hematopoietic system was reconstituted into *Spns2*[tm1a/tm1a] hosts, the numbers of T cells were depleted in the blood and spleen to the same extent as in *Spns2*[tm1a/tm1a] mice reconstituted with *Spns2*[tm1a/tm1a] bone marrow (Fig. 6). Similarly, mature B cells were depleted to an equal extent in both groups of mice in the blood, spleen, bone marrow (Supplemental Fig. 2). In contrast, in the chimeric mice with selective loss of Spns2 function in the hematopoietic compartment, there was a trend toward decreased lymphocyte numbers but this did not reach statistical significance (Fig. 6, Supplemental Fig. 2), further indicating that Spns2 is primarily functional in the nonhematopoietic cells. Overall, these data suggested that Spns2 expression and function on the cells of the nonhematopoietic stroma had a primary role in the maintenance of normal lymphocyte development and immune system function.

No significant reduction in the plasma S1P levels in Spns2[tm1a/tm1a] *mice*

S1P levels in the plasma of *Spns2*[tm1a/tm1a] and wild-type mice were measured using two methods, an ELISA-based S1P assay (Echelon Biosciences; Fig. 7A), and the S1P$_1$ redistribution assay that measures S1P-induced internalization of S1P$_1$ (Thermo Scientific; Fig. 7B, 7C). In the latter assay, the plasma of wild-type and *Spns2*[tm1a/tm1a] mice was added at different dilutions to U2OS cells expressing GFP-tagged S1P$_1$ and the internalization of S1P$_1$ GFP was quantified using a Cellomics Array-Scan VTI high-throughput cell imaging system. No significant differences in S1P concen-

trations or activity were observed between *Spns2*[tm1a/tm1a] and wild-type mice in either assay (Fig. 7A, 7C). This indicated that Spns2-independent mechanisms exist for maintaining overall S1P levels in the blood of *Spns2*[tm1a/tm1a] mice, but did not rule out the possibility that S1P levels are reduced in certain localized environments and that this was responsible for the altered lymphocyte distribution and immune function in *Spns2*[tm1a/tm1a] mice. Normal viability and lack of gross developmental defects in the *Spns2*[tm1a/tm1a] mice are also consistent with localized rather than systemic defects in S1P export. S1P concentrations in the lysates of spleen and thymus tissues were below the limit of detection of the Echelon Biosciences ELISA assay for both wild-type and *Spns2*[tm1a/tm1a] mice (<0.06 μM; data not shown).

Characterization of Spns2 *knockout* Spns2[tm1b/tm1b] *mice*

To further confirm that the *Spns2*[tm1a/tm1a] mice were phenotypically equivalent to *Spns2* knockout animals, the *Spns2*[tm1a/tm1a] line was crossed to the C57BL/6N-Hprt[Tg(CMV-cre)Brd/Wtsi] transgenic line with systemic expression of Cre recombinase (44). This resulted in germline excision of asymmetric exon 3 of the *Spns2* gene (Supplemental Fig. 3A), causing a frameshift in the *Spns2* transcript, and is therefore predicted to result in a full loss of Spns2 protein expression. Additionally, the removal of the β-actin promoter, contained in the neomycin cassette, controlled for any possible side effects of this cassette on the phenotype. The resulting allele structure was designated *Spns2*[tm1b(KOMP)Wtsi], and the homozygous *Spns2*[tm1b/tm1b] mice were viable with no significant increase in embryonic mortality. Flow cytometry analysis of lymphoid organs demonstrated a reduction in CD4 and CD8 T cells and mature B cells in the spleen of *Spns2*[tm1b/tm1b] mice (Supplemental Fig. 3B), comparable to *Spns2*[tm1a/tm1a] mice (Figs. 1A, 2A). There was also an increase in the proportion of CD4^{+}CD8^{−} and CD4^{−}CD8^{+} T cells in the thymus of *Spns2*[tm1b/tm1b]
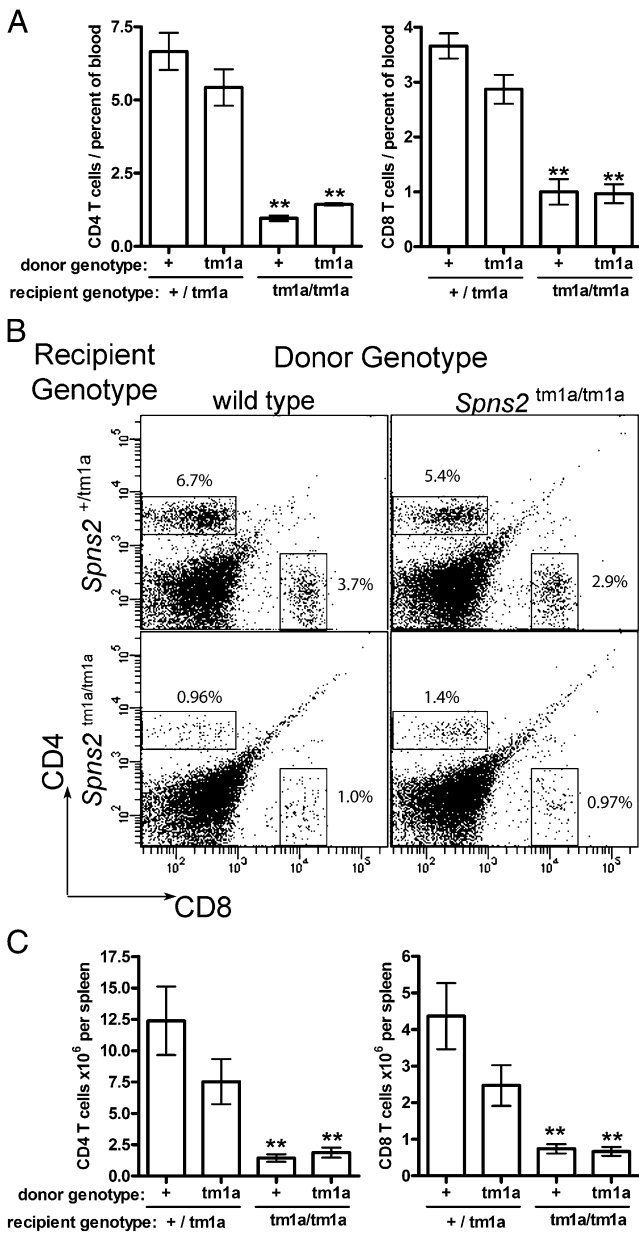
FIGURE 6. Bone marrow chimeras experiments indicate that Spns2 expression and function in the nonhematopoietic cells of the stoma is required for normal lymphocyte development. Lethally irradiated (2 × 4.5 Gy) recipients of $Spns2^{tm1a/tm1a}$ and $Spns2^{+/tm1a}$ genotypes were reconstituted either with wild-type (+) or with $Spns2^{tm1a/tm1a}$ (tm1a) donor bone marrow, and the numbers of lymphocyte subsets were analyzed by flow cytometry at 8 wk following reconstitution. (**A**) Percentage of CD4 and CD8 T cells in the blood of the chimeric mice of the four groups. (**B**) Representative flow cytometry plots of the blood of the chimeric mice, stained for CD4 and CD8; average percentages of cells within the gated populations are indicated. (**C**) Absolute numbers of CD4 and CD8 T cells in the spleen of the chimeric mice of the four groups. Bars represent means ± SEM from three or more mice per group; statistical comparisons were made using ANOVA with a Bonferroni post hoc test to compare each dataset to the control group. ** $p < 0.01$.

mice, and these cells expressed higher levels of CD62L and lower levels of CD24, indicating their more mature status (Supplemental Fig. 3B), as seen previously in $Spns2^{tm1a/tm1a}$ mice (Fig. 1B–E). Overall, this confirmed that the $Spns2^{tm1a/tm1a}$ phenotype is equivalent to the Spns2 knockout $Spns2^{tm1b/tm1b}$.

Additionally, to further confirm that the $Spns2^{tm1a/tm1a}$ phenotype resulted from the gene-trap cassette in the $Spns2$ locus, the
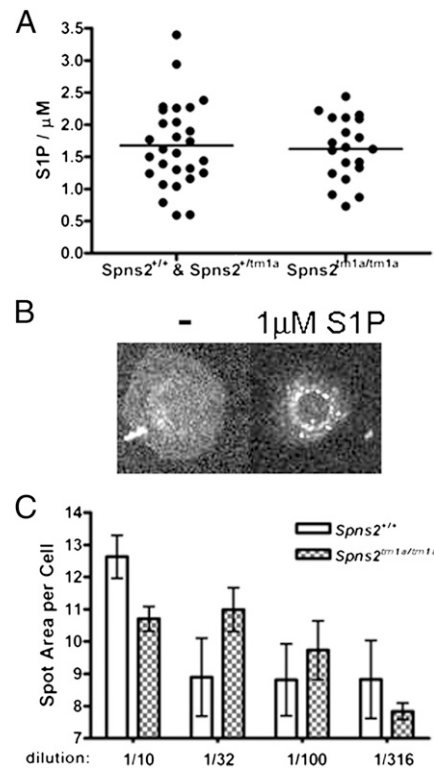

FIGURE 7. No significant alterations in the levels of S1P in the plasma of $Spns2^{tm1a/tm1a}$ mice. (**A**) S1P concentration in plasma measured using the ELISA-based S1P assay kit (from Echelon Biosciences). (**B**) Sample images of U2OS cells expressing GFP-tagged $S1P_1$ (Thermo Scientific) following exposure to media containing either no S1P or 1 μM S1P. The data were acquired using the Cellomics cell imaging system and show internalization of $S1P_1$ in the cells exposed to S1P. Original magnification ×20. (**C**) Cellomics system-based quantification of $S1P_1$-GFP internalization in U2OS cells exposed to wild type or $Spns2^{tm1a/tm1a}$ plasma at different dilutions. Quantification was performed using the spot detection algorithm and the spot total area per object function. Bars represent means ± SEM from four mice per group. The differences between wild-type and $Spns2^{tm1a/tm1a}$ samples are not statistically significant.

$Spns2^{tm1a/tm1a}$ animals were crossed to a transgenic line with systemic expression of Flp recombinase C57BL/6N-Gt(ROSA) 26Sor$^{tm1(FLP1)Dym/Wtsi}$ (45), causing germline excision of the gene-trap cassette (Supplemental Fig. 3A). The resulting allele was designated $Spns2^{tm1c(KOMP)Wtsi}$, and the $Spns2^{tm1c/tm1c}$ mice showed a rescue of lymphocyte numbers in the spleen, bone marrow, and thymus (Supplemental Fig. 3C and data not shown), confirming that the immune phenotype of the $Spns2^{tm1a/tm1a}$ line was caused by the $Spns2^{tm1a}$ gene-trap cassette.

Discussion

In this study, we have characterized an $Spns2$-targeted mouse line and demonstrated that Spns2 is required for normal lymphocyte development and localization, as well as for normal humoral immune response to immunization. Overall the changes in lymphocyte subpopulations in $Spns2^{tm1a/tm1a}$ and $Spns2^{tm1b/tm1b}$ mice closely mimicked the phenotypes of partial S1P deficiency and impaired S1P-dependent lymphocyte trafficking, including the depletion of lymphocytes in circulation, increase in the mature single-positive T cells in the thymus, and a selective reduction in the mature B cell population in the spleen and bone marrow (5, 6, 10, 31, 46). Although we did not detect a reduction in S1P levels in $Spns2^{tm1a/tma1}$ mouse plasma, the phenotypic data presented in this study together

with the previous in vitro demonstrations that human Spns2 can transport S1P and S1P mimic FTY720 (39, 42), suggest that the *Spns2*[tm1a/tm1a] phenotype may arise from localized disruptions in S1P concentrations at certain restricted physiological locations.

Critically, this work indicates that Spns2 functions are limiting for lymphocyte trafficking with some degree of specificity, as the viability and lack of developmental defects in *Spns2*[tm1a/tm1a] mice contrast with lethality and defects in cardiovascular and neural development in *Spns2*-mutant zebrafish (39, 40). Importantly, this is not due to different requirements for S1P production between the two species, as knockout mice lacking sphingosine kinases $SphK1^{-/-} SphK2^{-/-}$ or S1P receptor $S1P_1^{-/-}$ are also embryonic lethal with abnormal cardiovascular development (30, 41). In comparison, *Spns2*[tm1a/tm1a] mice more closely mimic the phenotypes of partially reduced S1P production, such as the single-null knockouts for *SphK1* or *SphK2* (53–55), or the knockout for S1P lyase with normal S1P production but disrupted S1P concentration gradients (56). Overall, this indicates that sufficient S1P levels are maintained in correct anatomical and cellular locations in the *Spns2*[tm1a/tm1a] mice to allow normal embryonic development, and it suggests significant divergence in the expression and functions of Spns2 between mice and zebrafish. We can speculate that alternative mechanisms of S1P release may operate during embryonic development in mouse but not in zebrafish species. These may include other proteins that have been shown to transport S1P in vitro in mammalian cells, such as ABCC1 and ABCA1 (32, 33), or extracellular S1P production by secreted SphK1 enzyme (37), or even the two Spns2 paralogs Spns1 and Spns3.

This work further demonstrated that Spns2 activity in the nonhematopoietic cells of the stroma is of key importance for normal immune system function. In contrast, previous studies showed that plasma S1P levels in the mouse are maintained by hematopoietic cells such as erythrocytes (46), and ABC family transporters have been implicated in mediating S1P export from erythrocytes (32) and platelets (34). This suggests that the primary role of Spns2 is to maintain appropriate S1P concentrations at other in vivo locations, consistent with the unaltered S1P levels in the plasma of *Spns2*[tm1a/tm1a] mice. Lymph is one of the sites where analysis of S1P concentrations would be particularly interesting (46), as S1P in the lymph was shown to be derived from nonhematopoietic cells, in particular the lymphatic endothelium (47). Overall, this warrants further investigation of Spns2 expression in different nonhematopoietic cell types and tissues, including lymphatic endothelium (46, 47).

S1P also acts as an intracellular messenger, and in mast cells and APCs increased S1P production is associated with cell activation, degranulation, and inflammatory cytokine production (18, 20, 23, 24). However, the present work indicates that in contrast to the *SphK1* knockdown cells, *Spns2*[tm1a/tm1a] macrophages respond normally to TNFR and TLR stimulation. This indicates that Spns2 likely does not affect intracellular S1P levels, at least in this cell type. Whether the activity of Spns2 and other S1P transporters can affect intracellular S1P levels in other cell types, by altering S1P secretion or uptake, remains to be addressed in future research.

Components of the S1P signaling pathways are targets for therapies aimed at treating autoimmunity, transplant rejection, inflammatory diseases, and cancer (2). The S1P receptor agonist FTY720 is the most advanced of such therapies and was recently approved for the treatment of multiple sclerosis (57). Other pharmaceutical agents are under development and have shown efficacy in animal models of inflammatory diseases, sepsis, and cancer (27, 58, 59). Knowledge of the mechanisms regulating S1P concentrations in vivo in a mammal is essential for the future development of such pharmaceutical agents and may lead to better targeted therapies. For example, S1P-targeting therapies for the treatment of autoimmunity and transplant rejection aim to achieve immunosuppression without inhibiting other S1P activities. S1P-targeting cancer therapies suppress vascularization, cell growth, and migration, but ideally they aim to maintain full immune system function. In contrast, therapies for systemic inflammatory disorders primarily aim to suppress inflammation and intravascular coagulation while retaining the protective activities of S1P on endothelial barrier integrity (60, 61). Given the diverse roles of S1P in many physiological processes, understanding the mechanisms regulating its bioavailability in different tissues and under different conditions is essential for the development of such therapies. Transporter proteins have proven highly effective drug targets in other areas, particularly neuropharmacology (62). The demonstration that *Spns2* deficiency selectively impaired lymphocyte functions and Ag-specific immune responses, without affecting vascular and neural development, highlights Spns2 as a possible drug target with potential for the treatment of autoimmunity and transplant rejection.

While this manuscript was under review, another study was published that substantially agrees with many of the findings presented in our study (63).

References

1. Fyrst, H., and J. D. Saba. 2010. An update on sphingosine-1-phosphate and other sphingolipid mediators. *Nat. Chem. Biol.* 6: 489–497.
2. Japtok, L., and B. Kleuser. 2009. The role of sphingosine-1-phosphate receptor modulators in the prevention of transplant rejection and autoimmune diseases. *Curr. Opin. Investig. Drugs* 10: 1183–1194.
3. Rosen, H., P. J. Gonzalez-Cabrera, M. G. Sanna, and S. Brown. 2009. Sphingosine 1-phosphate receptor signaling. *Annu. Rev. Biochem.* 78: 743–768.
4. Rivera, J., R. L. Proia, and A. Olivera. 2008. The alliance of sphingosine-1-phosphate and its receptors in immunity. *Nat. Rev. Immunol.* 8: 753–763.
5. Matloubian, M., C. G. Lo, G. Cinamon, M. J. Lesneski, Y. Xu, V. Brinkmann, M. L. Allende, R. L. Proia, and J. G. Cyster. 2004. Lymphocyte egress from thymus and peripheral lymphoid organs is dependent on S1P receptor 1. *Nature* 427: 355–360.

6. Allende, M. L., J. L. Dreier, S. Mandala, and R. L. Proia. 2004. Expression of the sphingosine 1-phosphate receptor, S1P₁, on T-cells controls thymic emigration. *J. Biol. Chem.* 279: 15396–15401.

7. Allende, M. L., G. Tuymetova, B. G. Lee, E. Bonifacino, Y. P. Wu, and R. L. Proia. 2010. S1P₁ receptor directs the release of immature B cells from bone marrow into blood. *J. Exp. Med.* 207: 1113–1124.

8. Pereira, J. P., Y. Xu, and J. G. Cyster. 2010. A role for S1P and S1P₁ in immature-B cell egress from mouse bone marrow. *PLoS ONE* 5: e9277.

9. Mandala, S., R. Hajdu, J. Bergstrom, E. Quackenbush, J. Xie, J. Milligan, R. Thornton, G. J. Shei, D. Card, C. Keohane, et al. 2002. Alteration of lymphocyte trafficking by sphingosine-1-phosphate receptor agonists. *Science* 296: 346–349.

10. Schwab, S. R., and J. G. Cyster. 2007. Finding a way out: lymphocyte egress from lymphoid organs. *Nat. Immunol.* 8: 1295–1301.

11. Cinamon, G., M. A. Zachariah, O. M. Lam, F. W. Foss, Jr., and J. G. Cyster. 2008. Follicular shuttling of marginal zone B cells facilitates antigen transport. *Nat. Immunol.* 9: 54–62.

12. Kunisawa, J., Y. Kurashima, M. Gohda, M. Higuchi, I. Ishikawa, F. Miura, I. Ogahara, and H. Kiyono. 2007. Sphingosine 1-phosphate regulates peritoneal B-cell trafficking for subsequent intestinal IgA production. *Blood* 109: 3749–3756.

13. Kabashima, K., N. M. Haynes, Y. Xu, S. L. Nutt, M. L. Allende, R. L. Proia, and J. G. Cyster. 2006. Plasma cell S1P₁ expression determines secondary lymphoid organ retention versus bone marrow tropism. *J. Exp. Med.* 203: 2683–2690.

14. Kunisawa, J., Y. Kurashima, M. Higuchi, M. Gohda, I. Ishikawa, I. Ogahara, N. Kim, M. Shimizu, and H. Kiyono. 2007. Sphingosine 1-phosphate dependence in the regulation of lymphocyte trafficking to the gut epithelium. *J. Exp. Med.* 204: 2335–2348.

15. Walzer, T., L. Chiossone, J. Chaix, A. Calver, C. Carozzo, L. Garrigue-Antar, Y. Jacques, M. Baratin, E. Tomasello, and E. Vivier. 2007. Natural killer cell trafficking in vivo requires a dedicated sphingosine 1-phosphate receptor. *Nat. Immunol.* 8: 1337–1344.

16. Strub, G. M., M. Maceyka, N. C. Hait, S. Milstien, and S. Spiegel. 2010. Extracellular and intracellular actions of sphingosine-1-phosphate. *Adv. Exp. Med. Biol.* 688: 141–155.

17. Olivera, A. 2008. Unraveling the complexities of sphingosine-1-phosphate function: the mast cell model. *Prostaglandins Other Lipid Mediat.* 86: 1–11.

18. Florey, O., and D. O. Haskard. 2009. Sphingosine 1-phosphate enhances Fcγ receptor-mediated neutrophil activation and recruitment under flow conditions. *J. Immunol.* 183: 2330–2336.

19. Olivera, A., K. Mizugishi, A. Tikhonova, L. Ciaccia, S. Odom, R. L. Proia, and J. Rivera. 2007. The sphingosine kinase-sphingosine-1-phosphate axis is a determinant of mast cell function and anaphylaxis. *Immunity* 26: 287–297.

20. Prakash, H., A. Lüth, N. Grinkina, D. Holzer, R. Wadgaonkar, A. P. Gonzalez, E. Anes, and B. Kleuser. 2010. Sphingosine kinase-1 (SphK-1) regulates *Mycobacterium* smegmatis infection in macrophages. *PLoS ONE* 5: e10657.

21. Vlasenko, L. P., and A. J. Melendez. 2005. A critical role for sphingosine kinase in anaphylatoxin-induced neutropenia, peritonitis, and cytokine production in vivo. *J. Immunol.* 174: 6456–6461.

22. Ibrahim, F. B., S. J. Pang, and A. J. Melendez. 2004. Anaphylatoxin signaling in human neutrophils. A key role for sphingosine kinase. *J. Biol. Chem.* 279: 44802–44811.

23. Choi, O. H., J. H. Kim, and J. P. Kinet. 1996. Calcium mobilization via sphingosine kinase in signalling by the FcεRI antigen receptor. *Nature* 380: 634–636.

24. Prieschl, E. E., R. Csonga, V. Novotny, G. E. Kikuchi, and T. Baumruker. 1999. The balance between sphingosine and sphingosine-1-phosphate is decisive for mast cell activation after Fcε receptor I triggering. *J. Exp. Med.* 190: 1–8.

25. Alvarez, S. E., K. B. Harikumar, N. C. Hait, J. Allegood, G. M. Strub, E. Y. Kim, M. Maceyka, H. Jiang, C. Luo, T. Kordula, et al. 2010. Sphingosine-1-phosphate is a missing cofactor for the E3 ubiquitin ligase TRAF2. *Nature* 465: 1084–1088.

26. Niessen, F., F. Schaffner, C. Furlan-Freguia, R. Pawlinski, G. Bhattacharjee, J. Chun, C. K. Derian, P. Andrade-Gordon, H. Rosen, and W. Ruf. 2008. Dendritic cell PAR1-S1P3 signalling couples coagulation and inflammation. *Nature* 452: 654–658.

27. Lai, W. Q., A. W. Irwan, H. H. Goh, H. S. Howe, D. T. Yu, R. Valle-Oñate, I. B. McInnes, A. J. Melendez, and B. P. Leung. 2008. Anti-inflammatory effects of sphingosine kinase modulation in inflammatory arthritis. *J. Immunol.* 181: 8010–8017.

28. Pitson, S. M., R. J. D'andrea, L. Vandeleur, P. A. Moretti, P. Xia, J. R. Gamble, M. A. Vadas, and B. W. Wattenberg. 2000. Human sphingosine kinase: purification, molecular cloning and characterization of the native and recombinant enzymes. *Biochem. J.* 350: 429–441.

29. Liu, H., M. Sugiura, V. E. Nava, L. C. Edsall, K. Kono, S. Poulton, S. Milstien, T. Kohama, and S. Spiegel. 2000. Molecular cloning and functional characterization of a novel mammalian sphingosine kinase type 2 isoform. *J. Biol. Chem.* 275: 19513–19520.

30. Mizugishi, K., T. Yamashita, A. Olivera, G. F. Miller, S. Spiegel, and R. L. Proia. 2005. Essential role for sphingosine kinases in neural and vascular development. *Mol. Cell. Biol.* 25: 11113–11121.

31. Schwab, S. R., J. P. Pereira, M. Matloubian, Y. Xu, Y. Huang, and J. G. Cyster. 2005. Lymphocyte sequestration through S1P lyase inhibition and disruption of S1P gradients. *Science* 309: 1735–1739.

32. Mitra, P., C. A. Oskeritzian, S. G. Payne, M. A. Beaven, S. Milstien, and S. Spiegel. 2006. Role of ABCC1 in export of sphingosine-1-phosphate from mast cells. *Proc. Natl. Acad. Sci. USA* 103: 16394–16399.

33. English, D., Z. Welch, A. T. Kovala, K. Harvey, O. V. Volpert, D. N. Brindley, and J. G. Garcia. 2000. Sphingosine 1-phosphate released from platelets during clotting accounts for the potent endothelial cell chemotactic activity of blood

34. Kobayashi, N., T. Nishi, T. Hirata, A. Kihara, T. Sano, Y. Igarashi, and A. Yamaguchi. 2006. Sphingosine 1-phosphate is released from the cytosol of rat platelets in a carrier-mediated manner. *J. Lipid Res.* 47: 614–621.

35. Boujaoude, L. C., C. Bradshaw-Wilder, C. Mao, J. Cohn, B. Ogretmen, Y. A. Hannun, and L. M. Obeid. 2001. Cystic fibrosis transmembrane regulator regulates uptake of sphingoid base phosphates and lysophosphatidic acid: modulation of cellular activity of sphingosine 1-phosphate. *J. Biol. Chem.* 276: 35258–35264.

36. Lee, Y. M., K. Venkataraman, S. I. Hwang, D. K. Han, and T. Hla. 2007. A novel method to quantify sphingosine 1-phosphate by immobilized metal affinity chromatography (IMAC). *Prostaglandins Other Lipid Mediat.* 84: 154–162.

37. Ancellin, N., C. Colmont, J. Su, Q. Li, N. Mittereder, S. S. Chae, S. Stefansson, G. Liau, and T. Hla. 2002. Extracellular export of sphingosine kinase-1 enzyme. Sphingosine 1-phosphate generation and the induction of angiogenic vascular maturation. *J. Biol. Chem.* 277: 6667–6675.

38. Saier, M. H., Jr., J. T. Beatty, A. Goffeau, K. T. Harley, W. H. Heijne, S. C. Huang, D. L. Jack, P. S. Jähn, K. Lew, J. Liu, et al. 1999. The major facilitator superfamily. *J. Mol. Microbiol. Biotechnol.* 1: 257–279.

39. Kawahara, A., T. Nishi, Y. Hisano, H. Fukui, A. Yamaguchi, and N. Mochizuki. 2009. The sphingolipid transporter Spns2 functions in migration of zebrafish myocardial precursors. *Science* 323: 524–527.

40. Osborne, N., K. Brand-Arzamendi, E. A. Ober, S. W. Jin, H. Verkade, N. G. Holtzman, D. Yelon, and D. Y. Stainier. 2008. The spinster homolog, two of hearts, is required for sphingosine 1-phosphate signaling in zebrafish. *Curr. Biol.* 18: 1882–1888.

41. Liu, Y., R. Wada, T. Yamashita, Y. Mi, C. X. Deng, J. P. Hobson, H. M. Rosenfeldt, V. E. Nava, S. S. Chae, M. J. Lee, et al. 2000. Edg-1, the G protein-coupled receptor for sphingosine-1-phosphate, is essential for vascular maturation. *J. Clin. Invest.* 106: 951–961.

42. Hisano, Y., N. Kobayashi, A. Kawahara, A. Yamaguchi, and T. Nishi. 2011. The sphingosine 1-phosphate transporter, SPNS2, functions as a transporter of the phosphorylated form of the immunomodulating agent FTY720. *J. Biol. Chem.* 286: 1758–1766.

43. Skarnes, W. C., B. Rosen, A. P. West, M. Koutsourakis, W. Bushell, V. Iyer, A. O. Mujica, M. Thomas, J. Harrow, T. Cox, et al. 2011. A conditional knockout resource for the genome-wide study of mouse gene function. *Nature* 474: 337–342.

44. Su, H., A. A. Mills, X. Wang, and A. Bradley. 2002. A targeted X-linked CMV-Cre line. *Genesis* 32: 187–188.

45. Farley, F. W., P. Soriano, L. S. Steffen, and S. M. Dymecki. 2000. Widespread recombinase expression using FLPeR (flipper) mice. *Genesis* 28: 106–110.

46. Pappu, R., S. R. Schwab, I. Cornelissen, J. P. Pereira, J. B. Regard, Y. Xu, E. Camerer, Y. W. Zheng, Y. Huang, J. G. Cyster, and S. R. Coughlin. 2007. Promotion of lymphocyte egress into blood and lymph by distinct sources of sphingosine-1-phosphate. *Science* 316: 295–298.

47. Pham, T. H. M., P. Baluk, Y. Xu, I. Grigorova, A. J. Bankovich, R. Pappu, S. R. Coughlin, D. M. McDonald, S. R. Schwab, and J. G. Cyster. 2010. Lymphatic endothelial cell sphingosine kinase activity is required for lymphocyte egress and lymphatic patterning. *J. Exp. Med.* 207: 17–27.

48. Venkataraman, K., Y. M. Lee, J. Michaud, S. Thangada, Y. Ai, H. L. Bonkovsky, N. S. Parikh, C. Habrukowich, and T. Hla. 2008. Vascular endothelium as a contributor of plasma sphingosine 1-phosphate. *Circ. Res.* 102: 669–676.

49. Ito, K., Y. Anada, M. Tani, M. Ikeda, T. Sano, A. Kihara, and Y. Igarashi. 2007. Lack of sphingosine 1-phosphate-degrading enzymes in erythrocytes. *Biochem. Biophys. Res. Commun.* 357: 212–217.

50. Hänel, P., P. Andréani, and M. H. Gräler. 2007. Erythrocytes store and release sphingosine 1-phosphate in blood. *FASEB J.* 21: 1202–1209.

51. Adams, N. C., and N. W. Gale. 2006. High resolution gene expression analysis in mice using genetically inserted reporter genes. In *Mammalian and Avian Transgenesis—New Approaches*. S. Pease, and C. Lois, eds. Springer, Berlin, p. 131–173.

52. Nijnik, A., S. Clare, C. Hale, K. Yusa, A. R. Everitt, C. R. Raisen, L. Mottram, C. Podrini, M. Lucas, J. Estabel, et al; Sanger Institute Microarray Facility; Sanger Mouse Genetics Project. 2012. The critical role of histone H2A-deubiquitinase Mysm1 in hematopoiesis and lymphocyte differentiation. *Blood* 119: 1370–1379.

53. Allende, M. L., T. Sasaki, H. Kawai, A. Olivera, Y. Mi, G. van Echten-Deckert, R. Hajdu, M. Rosenbach, C. A. Keohane, S. Mandala, et al. 2004. Mice deficient in sphingosine kinase 1 are rendered lymphopenic by FTY720. *J. Biol. Chem.* 279: 52487–52492.

54. Kharel, Y., S. Lee, A. H. Snyder, S. L. Sheasley-O'neill, M. A. Morris, Y. Setiady, R. Zhu, M. A. Zigler, T. L. Burcin, K. Ley, et al. 2005. Sphingosine kinase 2 is required for modulation of lymphocyte traffic by FTY720. *J. Biol. Chem.* 280: 36865–36872.

55. Zemann, B., B. Kinzel, M. Müller, R. Reuschel, D. Mechtcheriakova, N. Urtz, F. Bornancin, T. Baumruker, and A. Billich. 2006. Sphingosine kinase type 2 is essential for lymphopenia induced by the immunomodulatory drug FTY720. *Blood* 107: 1454–1458.

56. Vogel, P., M. S. Donoviel, R. Read, G. M. Hansen, J. Hazlewood, S. J. Anderson, W. Sun, J. Swaffield, and T. Oravecz. 2009. Incomplete inhibition of sphingosine 1-phosphate lyase modulates immune system function yet prevents early lethality and non-lymphoid lesions. *PLoS ONE* 4: e4112.

57. Cohen, J. A., F. Barkhof, G. Comi, H. P. Hartung, B. O. Khatri, X. Montalban, J. Pelletier, R. Capra, P. Gallo, G. Izquierdo, et al; TRANSFORMS Study Group. 2010. Oral fingolimod or intramuscular interferon for relapsing multiple sclerosis. *N. Engl. J. Med.* 362: 402–415.

58. Milstien, S., and S. Spiegel. 2006. Targeting sphingosine-1-phosphate: a novel avenue for cancer therapeutics. *Cancer Cell* 9: 148–150.

59. Visentin, B., J. A. Vekich, B. J. Sibbald, A. L. Cavalli, K. M. Moreno, R. G. Matteo, W. A. Garland, Y. Lu, S. Yu, H. S. Hall, et al. 2006. Validation of an anti-sphingosine-1-phosphate antibody as a potential therapeutic in reducing growth, invasion, and angiogenesis in multiple tumor lineages. *Cancer Cell* 9: 225–238.

60. Rosen, H., M. G. Sanna, S. M. Cahalan, and P. J. Gonzalez-Cabrera. 2007. Tipping the gatekeeper: S1P regulation of endothelial barrier function. *Trends Immunol.* 28: 102–107.

61. Feistritzer, C., and M. Riewald. 2005. Endothelial barrier protection by activated protein C through PAR1-dependent sphingosine 1-phosphate receptor-1 cross-activation. *Blood* 105: 3178–3184.

62. Torres, G. E., R. R. Gainetdinov, and M. G. Caron. 2003. Plasma membrane monoamine transporters: structure, regulation and function. *Nat. Rev. Neurosci.* 4: 13–25.

63. Fukuhara, S., S. Simmons, S. Kawamura, A. Inoue, Y. Orba, T. Tokudome, Y. Sunden, Y. Arai, K. Moriwaki, J. Ishida, et al. 2012. The sphingosine-1-phosphate transporter Spns2 expressed on endothelial cells regulates lymphocyte trafficking in mice. *J. Clin. Invest.* 122: 1416–1426.

<p style="text-align:center">Supplementary Figures and Table</p>

The Role of Sphingosine-1-phosphate Transporter *Spns2* in Immune System Function

Anastasia Nijnik, Simon Clare, Christine Hale, Jing Chen, Claire Raisen, Lynda Mottram, Mark Lucas, Jeanne Estabel, Edward Ryder, Hibret Adissu, Sanger Mouse Genetics Project, Niels C. Adams, Ramiro Ramirez-Solis, Jacqueline K. White, Karen P. Steel, Gordon Dougan, and Robert E.W. Hancock

Figure S1. Characterization of *Spns2*[tm1a/tm1a] mouse phenotype. (A) Reduced white blood cell counts in *Spns2*[tm1a/tm1a] mice. Bars represent means ± SD, shaded areas represent 95% reference range for all wild type mice of same strain and sex. Blood was collected from terminally anaesthetized mice at 14 weeks of age into EDTA-coated tubes via the retro-orbital sinus, and analyzed on a ScilVet Animal Blood Counter. This data, together with the measurements of the percentages of the different lymphoid subpopulation in the blood (Figures 2A and 3A), indicated ~9.3 fold reduction in the absolute numbers of CD8 T cells, ~7.8 fold reduction in CD4 T cells, and ~3.9 fold reduction in B cells (CD19^{+}) in the blood of *Spns2*[tm1a/tm1a] versus wild type mice. (B) Normal responses of *Spns2*[tm1a/tm1a] bone marrow derived macrophages (BMDM) to challenges with inflammatory and microbial stimuli. *Spns2*[tm1a/tm1a] and wild type cells were stimulated with LPS (100 ng/ml), IFNγ (25 ng/ml), and/or TNFα (25 ng/ml), over a 48 hour time-course. TNFα production was measured by ELISA at 4 hours of stimulation; expression of activation markers CD80 and CD86 was measured by flow cytometry at 4, 24, and 48 hours and no differences were seen at any time-points, data presented is from 48 hours. Bars represent means ± SEM, from 4 mice per group; MFI, mean fluorescence intensity.
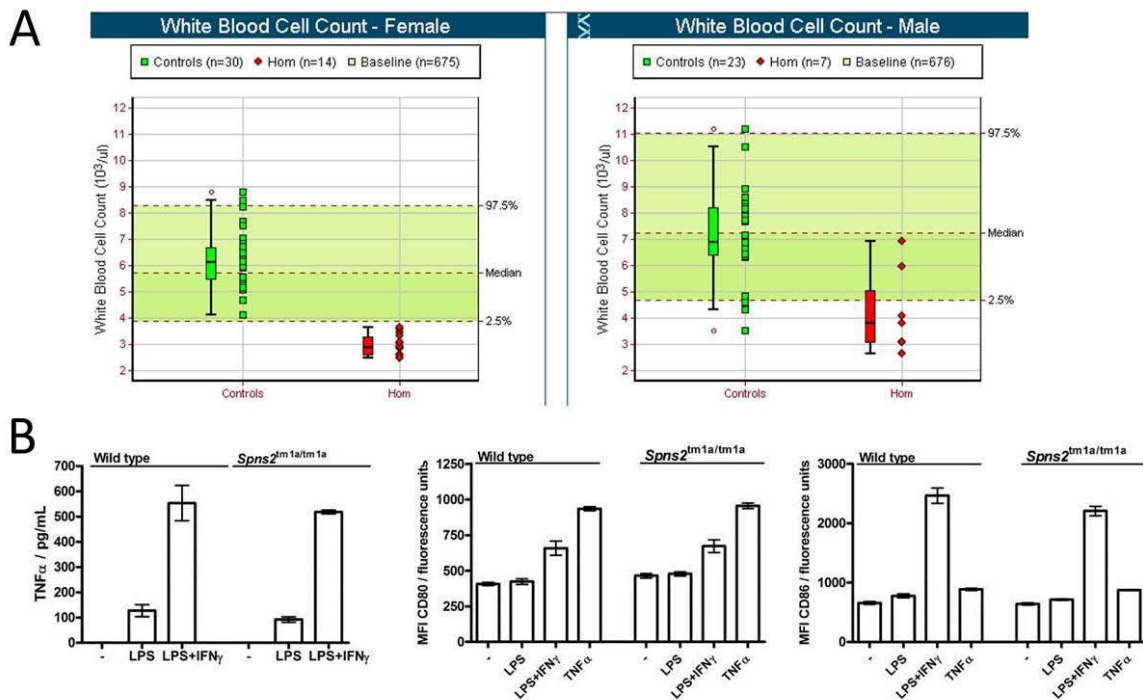
Figure S2. Bone marrow chimeras experiments indicate that Spns2 expression in the non-hematopoietic cells of the stoma is required for normal B cell development and localization. Lethally irradiated (2 x 4.5Gy) recipients of $Spns2^{tm1a/tm1a}$ and $Spns2^{+/tm1a}$ genotypes were reconstituted either with wild type (+) or with $Spns2^{tm1a/tm1a}$ (tm1a) donor bone marrow, and the numbers of lymphocyte subsets analyzed by flow cytometry at 8 weeks following reconstitution. (A) Numbers of transitional ($B220^+IgM^+IgD^-$) and mature ($B220^+IgM^+IgD^+$) B cells in the spleen of the chimeric mice. (B) Numbers of pre/pro-B cells ($B220^+IgM^-IgD^-$), immature ($B220^+IgM^+IgD^-$), and mature B cells ($B220^+IgM^+IgD^+$) in the bone marrow of the chimeric mice, per one tibia and femur. Means ± SEM from ≥3 mice per group are shown; statistical comparisons using ANOVA with Bonferroni's post-hoc test to compare each dataset to the control group; * $p<0.05$, **$p<0.01$.
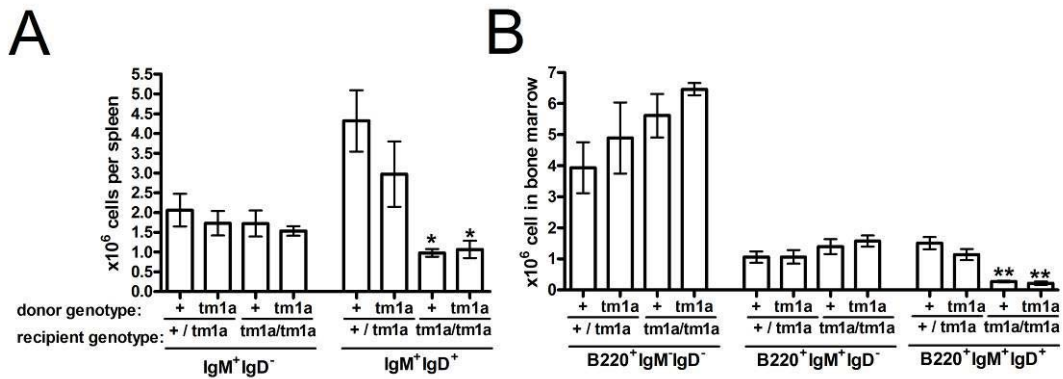
Figure S3. Characterization of *Spns2*[tm1b/tm1b] and *Spns2*[tm1c/tm1c] mouse phenotypes. (A) *Spns2*[tm1a] allele structure showing: (left) the LoxP-flanked region that is deleted by Cre-recombinase to produce the *Spns2*[tm1b] allele, lacking exon 3 and predicted to cause a frame-shift in the transcript and full loss of gene function; (right) the FRT-flanked region that is deleted by Flp-recombinase to produce the *Spns2*[tm1c] allele, lacking the splice-acceptor cassette and predicted to allow normal expression of wild type *Spns2*-transcript. (B) Numbers of T and B cell populations in the spleen, percentages of single positive CD4 and CD8 thymocytes in the thymus, and the expression of CD62L and CD24 markers on the single-positive thymocytes of wild type (+/+) and *Spns2*[tm1b/tm1b] (b/b) mice. (C, left) Numbers of CD4 and CD8 T cells in the spleen of *Spns2*[tm1c/tm1c] (c/c) mice; numbers in the control groups are also shown, including wild type (+/+), *Spns2*[tm1a/tm1a] (a/a), and heterozygous (+/a and +/c) animals. (C, right) Numbers of pre/pro-B cells (B220$^+$IgM$^-$IgD$^-$), immature B cells (B220$^+$IgM$^+$IgD$^-$), and mature B cells (B220$^+$IgM$^+$IgD$^+$) in the bone marrow and spleen of *Spns2*[tm1c/tm1c] (c/c), as compared to wild type (+/+) and heterozygous (+/c) mice. Equivalent data from *Spns2*[tm1a/tm1a] (a/a) animals is presented in Figures 3B,E. Bars represent means ± SEM from ≥3 mice per group; bone marrow cell counts per one tibia and femur; statistical comparisons using t-test or ANOVA with Bonferroni's post-hoc test; *p<0.05, **p<0.01, ***p<0.001; MFI – mean fluorescence intensity.
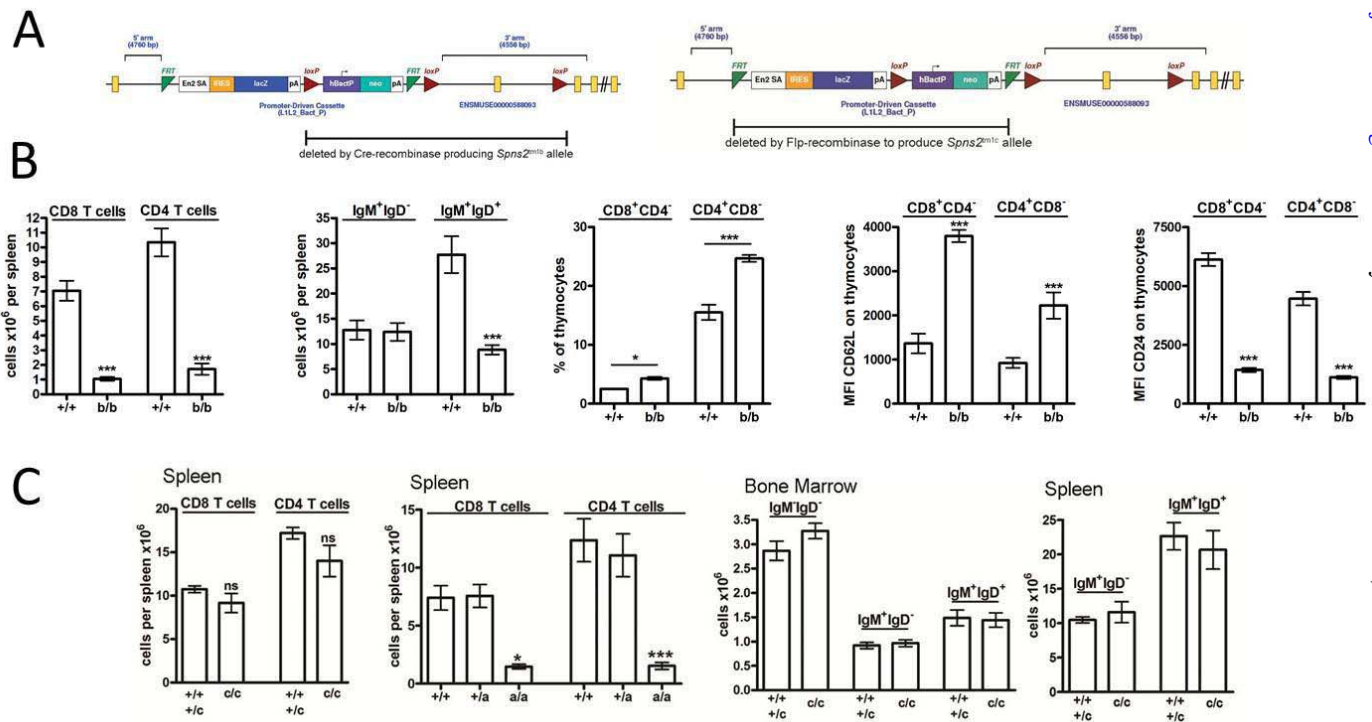
Table S1. Activity of the *Spns2*-promoter-driven *β*-galactosidase reporter in the tissues and organs of *Spns2*[tm1a/+] mice; data from three animals. *β*-galactosidase staining cannot be quantitatively compared across tissues and animals, and therefore "+" and "-" are used to indicate presence or absence of staining. The term 'no data' was assigned if the organ was not available. The term 'ambiguous' indicates uncertainty as to the validity of the observed pattern (staining may be very faint, background, or an artifact due to trapping).

Genotype	*Spns2*[tm1a]/+	*Spns2*[tm1a]/+
Gender	Female	Males
Age in Weeks	8.5	8.5 and 10.4
Adrenal Gland	-	-
Bone	+	+
Brain	+	+
Brown Adipose Tissue	-	-
Cartilage	-	-
Colon	-	-
Eye	-	+
Gall Bladder	*no data*	-
Heart	-	-
Kidney	+	+
Large Intestine	-	-
Liver	+	+
Lung	-	-
Mammary Gland	-	-
Mesenteric Lymph Node	+	+
Nasal Epithelia	-	-
Oesophagus	+	+
Oral Epithelia	+	+
Ovary	-	*no data*
Oviduct	+	*no data*
Pancreas	-	-
Peripheral Nervous System	-	-
Peyer's Patch	+	+
Pituitary Gland	*no data*	-
Prostate	*no data*	-
Skeletal Muscle	-	-
Skin	+	+
Small Intestine	-	-
Spinal Cord	+	+
Spleen	-	*ambiguous*
Stomach	+	+
Testis	*no data*	+
Thymus	-	-
Thyroid	*no data*	-
Trachea	-	-
Urinary System	+	+
Vas Deferens	*no data*	*ambiguous*
Vascular System	-	-
White Adipose Tissue	-	-